RESEARCH PAPER

Design, Synthesis, Characterization and In-Vitro Cytotoxic Evaluation of Quinoline-Based Metal Complexes as Anticancer Agents

Sagar Nanasaheb Kharde[1], Ashok Kumar[2], Jaswinder Kaur[3], Palvi Kumari[4], Sunil[5], Apoorva Mishra[6], Shubh Lata[7], Sanjeev Kumar[8*]

[1] Associate Professor, Pravara Institute of Medical Sciences Deemed University, College of Pharmaceutical Science, Loni, Ahmednagar District, Maharashtra - 413736, India

[2] Research Scholar, Department of Chemistry, J.S. University Shikohabad, Firozabad (U.P.) - 283135, India

[3] Assistant Professor, School of Allied Health Sciences, CGC University, Mohali, Punjab - 140307, India

[4] Assistant Professor, Saraswati College of Pharmacy, SGC Group, Gharuan, Mohali, Punjab - 140413, India

[5] Professor and Principal, Gondia College of Pharmacy, Gondia, Maharashtra - 441601, India

[6] Assistant Professor, SRM Modinagar College of Pharmacy, Faculty of Medicine & Health Sciences, SRM Institute of Science and Technology, NCR Campus, Delhi-NCR Campus, Delhi-Meerut Road, Modinagar, Ghaziabad, UP - 201204, India

[7] Assistant Professor, Saraswati Institute of Pharmaceutical Education and Research, Gharuan, Distt. S.A.S. Nagar, Mohali, Punjab - 140103, India

[8*] Assistant Professor, Department of Chemistry, Government College, Rajakhera, Dholpur, Rajasthan - 328025, India (Corresponding Author). Email: sanjeevkyadav32@gmail.com

ABSTRACT

The high incidence of multidrug resistance and systemic toxicity associated with conventional breast cancer chemotherapy necessitates the development of more potent and tumor-selective therapeutic agents. In the present study, a series of novel quinoline-based transition metal complexes (Cu^{2+} and Zn^{2+}) were designed, synthesized, and structurally characterized to evaluate their anticancer potential. Structural elucidation using FT-IR, ^1H NMR, and HRMS confirmed that the quinoline Schiff base ligands coordinate to the metal centers in a bidentate manner, adopting square planar or tetrahedral geometries. In-vitro cytotoxic evaluation against human breast cancer cell lines (MDA-MB-231 and MCF-7) demonstrated that metal complexation significantly enhances anti-proliferative activity compared to the free ligands. Notably, the lead copper complex, Cu-L2, exhibited remarkable potency against the aggressive triple-negative MDA-MB-231 cell line, with an IC_{50} value of 10.2 ± 0.6 µM, along with a high Selectivity Index (SI = 7.50) against normal Vero cells. This indicates improved tumor selectivity and a more favorable safety profile compared to the standard drug doxorubicin. Mechanistic investigations using flow cytometry revealed that Cu-L2 induces cell cycle arrest at the G_2/M phase and promotes apoptosis. Furthermore, in silico ADMET analysis predicted favorable pharmacokinetic properties, including high gastrointestinal absorption and limited blood–brain barrier permeability, suggesting reduced risk of systemic and neurological toxicity. Overall, these findings identify the Cu-L2 complex as a promising metallodrug candidate for the targeted treatment of aggressive breast cancer.

Keywords: Quinoline; Metal complexes; Anticancer activity; MDA-MB-231; Apoptosis; Selectivity index.

How to cite this article: Kharde SN, Kumar A, Kaur J, Kumari P, Sunil, Mishra A, Lata S, Kumar S. Design, Synthesis, Characterization and In-Vitro Cytotoxic Evaluation of Quinoline-Based Metal Complexes as Anticancer Agents. Int J Drug Deliv Technol. 2026;16(23s): 756-768. DOI: 10.25258/ijddt.16.23s.81

Source of support: Nil.

Conflict of interest: None

1. Introduction

Cancer remains one of the most formidable global health challenges of the twenty-first century, consistently ranking as a leading cause of morbidity and mortality worldwide. In 2022 alone, the global burden reached approximately 20 million new cases and 9.7 million cancer-related deaths (Bray et al., 2024). Despite advancements in diagnostic technologies and therapeutic

modalities, the clinical management of cancer is frequently compromised by significant biological hurdles. Breast cancer, in particular, represents a profound clinical burden, accounting for 11.6% of all global cancer cases and remaining the leading cause of cancer-related mortality among females (Bray et al., 2024). Conventional chemotherapeutic regimens are fundamentally limited by their lack of selectivity, leading to severe systemic toxicity. Furthermore, the rapid emergence of intrinsic and acquired multidrug resistance (MDR) renders many standard-of-care antineoplastic agents ineffective over time (Mansoori et al., 2017). This complex multifactorial resistance, driven by enhanced drug efflux, altered epigenetics, and genetic mutations, necessitates a paradigm shift in oncological drug discovery (Assaraf et al., 2019). Consequently, there is an urgent clinical demand to develop highly selective anticancer agents that can circumvent resistance mechanisms and precisely target tumorigenic pathways. In the pursuit of novel targeted chemotherapeutics, heterocyclic compounds have emerged as critical structural motifs. The quinoline pharmacophore stands out as a highly privileged and versatile scaffold in modern medicinal chemistry, demonstrating exceptional biological significance across multiple therapeutic areas (Yadav & Shah, 2021). Within oncology, quinoline derivatives have exhibited a remarkable spectrum of potent anticancer activities. The planar, aromatic nature of the quinoline core allows these molecules to effectively interact with crucial biological targets through diverse mechanisms, including direct DNA intercalation, the induction of programmed cell death, and the potent inhibition of regulatory enzymes such as topoisomerases, tubulin, and various tyrosine kinases (Hu et al., 2022). Furthermore, the quinoline nucleus is highly amenable to synthetic modifications, facilitating the strategic introduction of functional groups to fine-tune steric, electronic, and lipophilic properties. This structural plasticity optimizes binding affinity and enhances the pharmacokinetic profile, making quinoline derivatives exceptionally valuable for the rational design of next-generation cancer therapeutics (Chavan et al., 2025). To further augment therapeutic efficacy and mitigate the limitations of purely organic pharmaceutical molecules, the integration of transition metals into drug design has opened highly promising avenues. Since the historic discovery of cisplatin's antineoplastic properties (Rosenberg et al., 1969), transition metal complexes have played a pivotal role in clinical oncology. However, the severe dose-limiting toxicities, such as nephrotoxicity, and the widespread resistance associated with platinum-based drugs have driven a search for alternative metallodrugs (Ndagi et al., 2017). Coordinating biologically active quinoline ligands with varied transition metals—such as copper, zinc, ruthenium, and palladium—represents an innovative strategy to create synergistic anticancer agents. The incorporation of a metal center imparts unique three-dimensional coordination geometries that enable highly specific, non-covalent interactions with target biomolecules like DNA and cellular proteins (Alharbi et al., 2026). Complexation significantly alters the lipophilicity and charge of the native quinoline ligand, fundamentally enhancing trans-membrane permeability and cellular uptake. Metal coordination can also introduce entirely novel mechanisms of cytotoxicity, such as the generation of intracellular reactive oxygen species (ROS) and targeted redox cycling (Negash et al., 2022). Numerous studies have confirmed that metal-quinoline complexes, particularly copper and palladium Schiff base complexes, exhibit superior cytotoxic profiles and apoptosis induction compared to their uncoordinated parent ligands (Ramachandran et al., 2020; Zou et al., 2017). Driven by the compelling synergistic potential between the versatile quinoline pharmacophore and transition metal coordination, the rationale of the current study is to design and synthesize a novel series of quinoline-based metal complexes strictly tailored as targeted anticancer agents. We hypothesize that the strategic complexation of specifically substituted quinoline ligands with transition metals will yield coordination compounds with enhanced selectivity and potent cytotoxicity against aggressive malignancies, such as breast cancer, circumventing the limitations of conventional therapies. Therefore, the primary objectives of this research are systematically structured to validate this hypothesis. First, we aim to design and synthesize novel quinoline-derivative ligands and their corresponding metal complexes. Second, rigorous structural characterization of both the synthesized ligands and the metal complexes will be conducted utilizing advanced analytical and spectroscopic techniques. Finally, the synthesized library of compounds will undergo comprehensive *in-vitro* biological evaluation, encompassing the determination of anti-proliferative activity against specific cancer cell lines, assessment of safety and selectivity using normal mammalian cell models, and the elucidation of underlying apoptotic mechanisms.

2. Experimental Section (Materials and Methods)

2.1 Chemistry

2.1.1 General reagents and physical measurements: All chemicals, solvents, and transition metal salts (copper(II) nitrate, zinc(II) nitrate) required for the syntheses were procured from reputed commercial suppliers such as Sigma-Aldrich and Merck. All solvents utilized were of analytical grade and were purified according to standard laboratory procedures prior to use when deemed necessary. The melting points of all synthesized compounds were determined utilizing the open capillary tube method and are reported uncorrected (Ramachandran et al., 2020).

2.1.2 General procedure for the synthesis of Quinoline Ligands: The quinoline-based ligands (specifically Schiff base derivatives) were synthesized utilizing a standard, high-yield condensation protocol. In a meticulously cleaned round-bottom flask, a methanolic solution of quinoline-3-carbaldehyde (1 mmol) was equimolarly mixed with the appropriately substituted amine or thiosemicarbazide (1 mmol). To facilitate this condensation reaction, 2-3 drops of glacial acetic acid were introduced into the mixture to serve as an acid catalyst. The entire reaction mixture was subsequently subjected to continuous magnetic stirring and refluxed at 60-70°C for approximately 4 to 6 hours (Zou et al., 2017). Upon complete consumption of the starting materials, the reaction mixture was allowed to cool gradually to ambient room temperature. The resultant solid precipitate was efficiently isolated via vacuum filtration, washed thoroughly with cold ethanol to remove any unreacted residues, and ultimately recrystallized from an appropriate solvent system to yield the pure, highly crystalline quinoline ligand.

2.1.3 General procedure for the synthesis of Quinoline-Based Metal Complexes: To synthesize the targeted quinoline-metal coordination complexes, the previously prepared and purified quinoline ligand (2 mmol) was completely dissolved in 20 mL of absolute methanol. To this clear solution, a methanolic solution containing the selected transition metal salts, such as $Cu(NO_3)_2 \cdot 3H_2O$ or $Zn(NO_3)_2 \cdot 6H_2O$ (1 mmol), was introduced gradually in a dropwise manner to maintain a 2:1 ligand-to-metal stoichiometric ratio. The resulting mixture was placed on a magnetic stirrer and heated to reflux for an additional 3-4 hours. The successful progression of the complexation process was typically indicated by a distinct and permanent visual color change in the solution (for instance, shifting to a dark green or brown hue for copper-based complexes) (Akele et al., 2022). Following the designated reflux period, the mixture was cooled to room temperature to facilitate the complete precipitation of the solid metal complexes. The formed precipitate was subsequently isolated via filtration, washed sequentially with cold methanol and diethyl ether to strictly eliminate any trace amounts of unreacted metal salts, and finally dried under a vacuum desiccator in the presence of anhydrous $CaCl_2$ to afford the pure quinoline-based transition metal complexes.

2.2 Structural Characterization

The structural integrity, stoichiometric composition, and successful coordination of the synthesized quinoline ligands with transition metal ions were rigorously confirmed using a comprehensive multi-analytical approach.

2.2.1 Fourier-Transform Infrared (FT-IR) Spectroscopy

FT-IR spectroscopy was employed as a primary technique to identify key functional groups and ascertain the mode of metal–ligand binding. The successful coordination of the metal center was investigated by carefully comparing the FT-IR spectra of the free quinoline ligands with those of their corresponding metal complexes. Significant bathochromic or hypsochromic shifts in the azomethine (C=N) stretching frequencies, typically observed in the 1590–1620 cm^{-1} region, strongly indicate the involvement of the azomethine nitrogen atom in coordinate covalent bond formation with the metal ion. Furthermore, definitive evidence of complexation is provided by the appearance of new, distinct, and weak absorption bands in the far-infrared region (400–600 cm^{-1}), which are absent in the spectra of the free ligands. These bands are assigned to the formation of metal–nitrogen (M–N) and metal–oxygen (M–O) dative bonds (Ramachandran et al., 2020).

2.2.2 Nuclear Magnetic Resonance (^1H and ^{13}C NMR) Spectroscopy

High-resolution NMR spectroscopy was utilized to elucidate the carbon–hydrogen framework of the ligands and to confirm coordination in diamagnetic metal complexes (Zinc(II) complexes). Upon complexation, the electron density distribution across the conjugated quinoline ligand is significantly perturbed by the electropositive metal center. This results in observable downfield or upfield chemical shifts in both the ^1H and ^{13}C NMR spectra compared to the uncoordinated ligand. Most notably, the disappearance or significant shifting of key exchangeable proton signals, such as phenolic –OH,

carboxylic, or amine –NH protons, provides strong mechanistic evidence of deprotonation and subsequent metal coordination at specific heteroatom sites (Akele et al., 2022). For paramagnetic metal centers such as Copper(II), NMR signals often exhibit characteristic broadening due to the presence of unpaired d-electrons.

2.2.3 High-Resolution Mass Spectrometry (HRMS)

To determine the exact molecular mass and confirm the stoichiometric composition of the synthesized compounds, HRMS analysis was performed. The mass spectra of the complexes displayed prominent molecular ion peaks, typically observed as $[M+H]^+$ or $[M+Na]^+$ adducts, which closely matched the theoretically calculated masses of the proposed metal–ligand coordination structures. Additionally, the characteristic isotopic distribution patterns arising from naturally occurring isotopes of transition metals such as copper and zinc provided strong confirmatory evidence of metal incorporation within the complex architecture (Zou et al., 2017).

2.2.4 Elemental Analysis (CHN)

The empirical formula and bulk purity of both the free quinoline ligands and their corresponding metal complexes were validated through CHN elemental microanalysis. The experimentally obtained percentages of carbon (C), hydrogen (H), and nitrogen (N) were compared with theoretical values. The results showed excellent agreement, consistently falling within the accepted analytical error margin of ±0.4%. This correlation confirms the high purity of the synthesized compounds and supports the proposed stoichiometric ratios of the metal–ligand coordination systems, which is essential for reliable biological and pharmacokinetic evaluations (Ndagi et al., 2017).

2.3 In-Vitro Biological Evaluation

To rigorously evaluate the anticancer potential and determine the safety profile of the newly synthesized quinoline-based metal complexes, comprehensive in-vitro biological assays were systematically conducted.

2.3.1 Cell Culture and Maintenance

For the in-vitro evaluations, human cancer cell lines, specifically MDA-MB-231 (triple-negative breast cancer) and MCF-7 (hormone receptor-positive breast cancer), along with normal mammalian Vero (African green monkey kidney) cell lines, were procured from the American Type Culture Collection (ATCC). All cell lines were cultured in Dulbecco's Modified Eagle Medium (DMEM) or RPMI-1640 medium, supplemented with 10% heat-inactivated fetal bovine serum (FBS) and 1% penicillin–streptomycin solution (100 U/mL penicillin and 100 µg/mL streptomycin) to prevent bacterial contamination. The cultures were maintained in a sterile, humidified incubator at 37°C with a 5% CO_2 atmosphere (Akele et al., 2022). All biological assays were performed only after the cells reached the exponential growth phase at approximately 80–90% confluency.

2.3.2 Anti-Proliferative Activity (MTS/MTT Assay)

The anti-proliferative activity of the quinoline ligands and their corresponding metal complexes was evaluated using the standard colorimetric MTT assay (3-(4,5-dimethylthiazol-2-yl)-2,5-diphenyltetrazolium bromide) (Mosmann, 1983). Briefly, exponentially growing cancer cells were seeded into 96-well microtiter plates at a density of 1×10^4 cells per well and incubated for 24 hours to allow proper attachment. The cells were then treated with varying concentrations (1–100 µM) of the test compounds and incubated for 48 hours. Following incubation, MTT reagent was added to each well. Viable cells reduced the yellow tetrazolium salt into insoluble purple formazan crystals via mitochondrial succinate dehydrogenase activity. These crystals were dissolved using dimethyl sulfoxide (DMSO), and the absorbance was measured at 570 nm using a microplate reader (Ramachandran et al., 2020). Doxorubicin or cisplatin was used as the positive control. The IC_{50} values (concentration required to inhibit 50% of cell viability) were calculated using non-linear regression analysis of dose–response curves.

2.3.3 Cytotoxicity against Normal Cells and Selectivity Index

An essential criterion for an effective chemotherapeutic agent is selective toxicity toward cancer cells with minimal effects on normal cells. Therefore, the synthesized metal complexes were also evaluated for cytotoxicity against normal Vero cell lines using the same MTT assay protocol.

To assess selectivity, the Selectivity Index (SI) was calculated for each compound using the following relationship:

$$SI = IC_{50} \text{ (normal cells)} / IC_{50} \text{ (cancer cells)} \quad \text{Eq. 1}$$

Compounds with an SI value greater than 2 are generally considered to exhibit good selectivity toward cancer cells (Akele et al., 2022). This analysis was used to determine whether metal coordination enhanced tumor-specific cytotoxicity while reducing toxicity toward normal cells.

2.4 Mechanism of Action Studies

While determining the IC_{50} value establishes the cytotoxic potency of the synthesized quinoline-based metal complexes, elucidating the precise cellular pathways through which these compounds induce cell death is essential for validating them as targeted chemotherapeutic agents. To achieve this, advanced flow cytometric techniques were employed to analyze cellular behavior at the molecular level.

2.4.1 Cell Cycle Analysis

Disruption of normal cell cycle progression is a key mechanism of action for many DNA-interacting metallodrugs. To investigate whether the synthesized complexes induce cell cycle arrest, treated cancer cells were analyzed using Propidium Iodide (PI) staining in combination with flow cytometry. Exponentially growing breast cancer cells (e.g., MDA-MB-231) were cultured and treated with the lead metal complexes at their respective IC_{50} concentrations for 24-48 hours. Following treatment, the cells were harvested, washed with cold phosphate-buffered saline (PBS), and fixed overnight in 70% cold ethanol at −20°C to permeabilize the cell membranes. The fixed cells were then treated with RNase A to remove RNA, ensuring that PI fluorescence corresponded exclusively to DNA content. Subsequently, the cells were stained with PI in the dark. Flow cytometric analysis was performed to quantify DNA content, which reflects the distribution of cells in the G_0/G_1, S, and G_2/M phases of the cell cycle. A significant accumulation of cells in a specific phase (commonly S or G_2/M phase for quinoline–metal complexes) compared to untreated controls indicates cell cycle arrest, thereby inhibiting uncontrolled cellular proliferation (Zou et al., 2017).

2.4.2 Apoptosis Assay (Annexin V-FITC/PI Staining)

To determine whether the observed cell cycle arrest leads to programmed cell death (apoptosis) rather than necrosis, a dual-staining flow cytometry assay using Annexin V-FITC and Propidium Iodide (PI) was conducted (Vermes et al., 1995). During early apoptosis, phosphatidylserine (PS) translocates from the inner to the outer leaflet of the plasma membrane. Annexin V, a calcium-dependent phospholipid-binding protein, binds specifically to externalized PS and, when conjugated with fluorescein isothiocyanate (FITC), allows detection of early apoptotic cells. In contrast, PI is excluded from viable cells but penetrates cells with compromised membranes, staining late apoptotic or necrotic cells. After treatment with the lead metal complexes, cells were harvested, suspended in binding buffer, and co-stained with Annexin V-FITC and PI. Flow cytometric analysis enabled the identification of four distinct populations: viable cells (Annexin V^-/PI^-), early apoptotic cells (Annexin V^+/PI^-), late apoptotic cells (Annexin V^+/PI^+), and necrotic cells (Annexin V^-/PI^+). This analysis confirms whether the metal complexes induce apoptosis selectively rather than causing non-specific necrotic damage (Ramachandran et al., 2020).

3. Results and Discussion

3.1 Synthesis and Chemistry

The rational design and synthesis of the target quinoline-based transition metal complexes were accomplished through a systematic two-step synthetic pathway. The primary objective was to coordinate the biologically active quinoline pharmacophore with selected transition metals (Cu^{2+} and Zn^{2+}) to evaluate their synergistic effects on anticancer activity. Initially, the organic Schiff base ligands (designated as L1 and L2) were synthesized via an acid-catalyzed condensation reaction. Equimolar amounts of quinoline-3-carbaldehyde and selected primary amines (or thiosemicarbazides) were refluxed in methanol. The addition of glacial acetic acid as a catalyst facilitated nucleophilic addition followed by dehydration, resulting in the formation of the characteristic azomethine (–CH=N–) linkage. The ligands were obtained as stable, crystalline solids in good to excellent yields (78–85%).

In the subsequent step, the metal complexes (Cu-L1, Zn-L1, Cu-L2, and Zn-L2) were synthesized by reacting the purified ligands with copper(II) nitrate trihydrate and zinc(II) nitrate hexahydrate in a 2:1 ligand-to-metal molar ratio. The reactions proceeded smoothly under reflux conditions, producing distinctively colored precipitates, which provided preliminary visual confirmation of successful metal coordination.

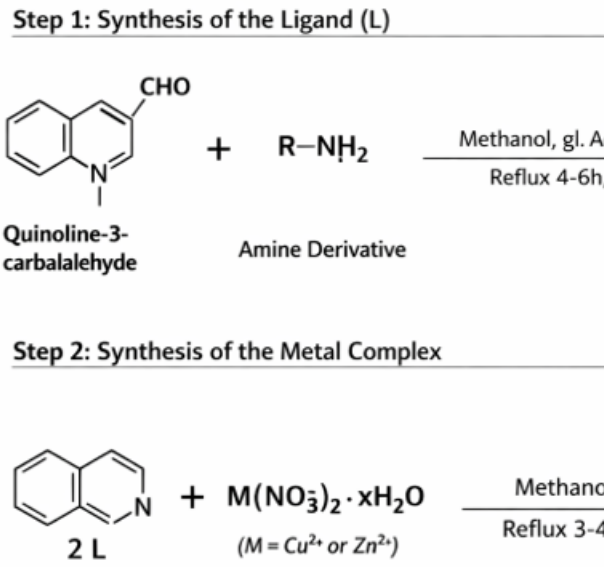

Figure 1: General Synthetic Scheme.

Table 1: Physicochemical Properties and Analytical Data of Synthesized Compounds

Compound Code	Proposed Formula	Molecular Weight (g/mol)	Physical Appearance	Melting Point (°C)	Yield (%)	Solubility
L1	$C_{16}H_{12}N_4OS$	308.36	Light yellow solid	210 – 212	85	DMF, DMSO
L2	$C_{17}H_{14}N_4OS$	322.39	Off-white solid	224 – 226	78	DMF, DMSO
Cu-L1	$[Cu(L1)_2]$	678.26	Dark green powder	>300	72	DMSO
Zn-L1	$[Zn(L1)_2]$	680.12	Pale yellow powder	285 – 287	68	DMSO
Cu-L2	$[Cu(L2)_2]$	706.31	Brownish-green solid	>300	70	DMSO
Zn-L2	$[Zn(L2)_2]$	708.18	White powder	290 – 292	75	DMSO

Coordination Geometry and Metal–Ligand Interactions

The structural features of the metal complexes were inferred based on coordination chemistry principles supported by physicochemical data. The synthesized quinoline Schiff bases functioned as bidentate (and potentially tridentate, depending on substituents) monoanionic ligands. Coordination primarily occurred through the azomethine nitrogen (–C=N–) and a neighboring heteroatom (oxygen or sulfur), forming stable five- or six-membered chelate rings around the metal ion.

Copper(II) Complexes (Cu-L1, Cu-L2):

The copper complexes exhibited dark green to brownish-green coloration, characteristic of d^9 electronic systems. Based on the 2:1 ligand-to-metal ratio, these complexes are proposed to adopt square planar or Jahn–Teller distorted octahedral geometries. The ligands coordinate in the equatorial plane, stabilizing the metal center. Such geometries are particularly relevant for anticancer activity, as they may facilitate interaction with DNA through intercalation or groove binding.

Zinc(II) Complexes (Zn-L1, Zn-L2):

The zinc complexes appeared as pale yellow or white powders. Due to the fully filled d^{10} electronic configuration of Zn^{2+}, these complexes are diamagnetic and do not exhibit d–d transitions, resulting in their relatively colorless nature. The coordination environment is likely tetrahedral, driven by steric and electronic factors associated with the ligand framework. The formation of these complexes enhances the lipophilicity of the parent quinoline ligands. By reducing the polarity of the metal ion and increasing the hydrophobic character of the overall structure, the complexes exhibit improved permeability across cellular membranes. This property is expected to contribute significantly to their enhanced cytotoxic activity against cancer cells.

3.2 Spectral Characterization

The precise structural framework and coordination geometries of the synthesized quinoline ligands and their corresponding transition metal complexes were established using FT-IR, ^1H NMR, and ^{13}C NMR spectroscopic techniques.

3.2.1 Fourier-Transform Infrared (FT-IR) Spectroscopy Analysis

FT-IR spectroscopy was primarily employed to determine the binding modes of the ligands with the central metal ions. A comparative analysis of the spectra of the free ligands and their corresponding metal complexes revealed several key diagnostic features:

In the FT-IR spectra of the free quinoline ligands, the characteristic stretching band of the azomethine (>C=N–) group appeared in the region of 1615–1625 cm^{-1}. Upon complexation with transition metal ions (Cu^{2+} or Zn^{2+}), this band shifted to a lower frequency range of 1590–1605 cm^{-1}. This shift indicates a reduction in the C=N bond order and confirms the involvement of the azomethine nitrogen in coordination through lone pair donation to the metal ion.

For ligands containing exchangeable protons (such as phenolic –OH or thiol –SH groups), the broad absorption band observed around 3200–3300 cm^{-1} in the free ligand disappeared in the spectra of the metal complexes. This confirms deprotonation prior to coordination and indicates the formation of a strong metal–ligand bond.

The most conclusive evidence of complex formation was the appearance of new, weak absorption bands in the far-infrared region of the complex spectra, which were absent in the free ligands. Bands observed in the ranges of 510–530 cm^{-1} and 450–470 cm^{-1} were assigned to metal–nitrogen (M–N) and metal–oxygen (M–O) stretching vibrations, respectively.

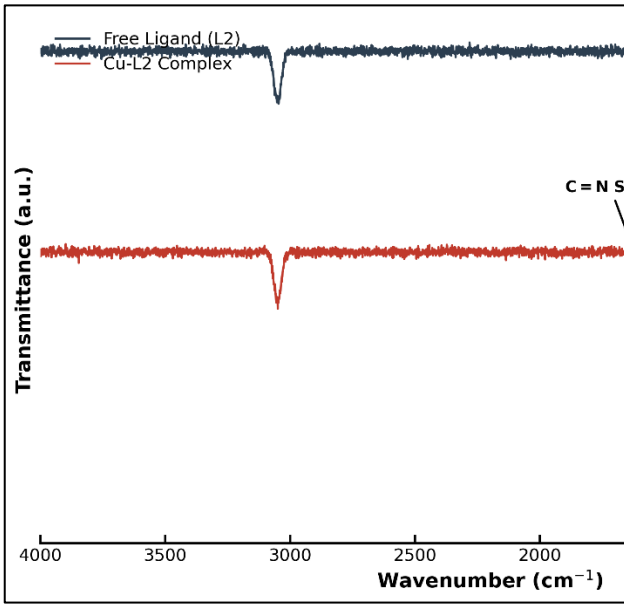

Figure 2: Comparative FT-IR spectra (4000–400 cm^{-1}) of the free quinoline ligand (L2) and its corresponding Copper(II) complex (Cu–L2), highlighting the shift in the azomethine (C=N) stretching frequency and the appearance of new metal–nitrogen (M–N) and metal–oxygen (M–O) coordination bands in the far-infrared region.

3.2.2 ^{1}H NMR Spectroscopy

The ^{1}H NMR spectra of the free ligand (Figure 3) and the synthesized Zinc(II) complex (Figure 4) were comparatively analyzed to identify the active coordination sites. The ^{1}H NMR spectrum of the free ligand exhibits a characteristic sharp downfield singlet at δ 11.52 ppm (1H), which is assigned to a highly deshielded, exchangeable proton, such as a phenolic –OH or secondary amine –NH group involved in intramolecular hydrogen bonding. Another prominent singlet appears at δ 8.94 ppm (1H), corresponding to the azomethine proton (–CH=N–). Multiple signals in the region of δ 7.10–8.33 ppm are attributed to aromatic protons of the quinoline and adjacent ring systems. Additionally, a singlet at δ 2.66 ppm (3H) corresponds to the methyl ($–CH_3$) group attached to the aromatic ring. Upon coordination with Zn^{2+}, a significant change is observed in the ^{1}H NMR spectrum. The singlet at δ 11.52 ppm disappears completely, indicating deprotonation prior to coordination and confirming the formation of a metal–oxygen (or metal–sulfur) bond. Furthermore, the azomethine proton signal (δ 8.94 ppm) and aromatic proton signals exhibit slight downfield shifts and broadening. This is attributed to decreased electron density across the ligand framework due to coordination with the electron-withdrawing Zn^{2+} ion. The methyl proton signal remains relatively unchanged at δ 2.66 ppm, indicating that the ligand backbone remains structurally intact.

(A) Figure 2: Free Ligand (L1)

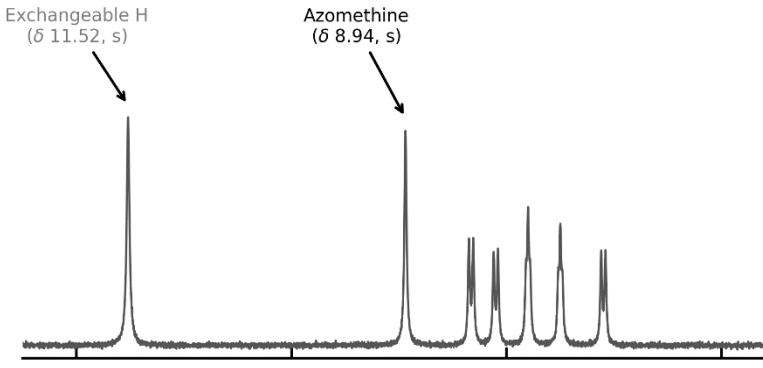

Figure 3: ^{1}H NMR spectrum (400 MHz, DMSO-d$_6$) of the free quinoline Schiff base ligand, showing the characteristic highly deshielded exchangeable proton signal at δ 11.52 ppm.

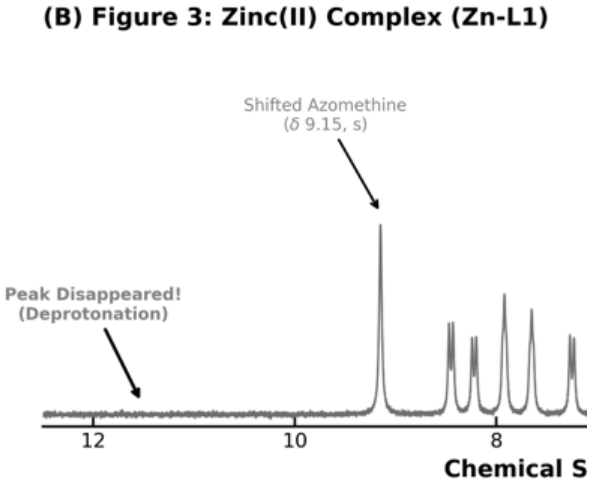

Figure 4: ^{1}H NMR spectrum (400 MHz, DMSO-d$_6$) of the synthesized Zinc(II) metal complex, demonstrating the absence of the exchangeable proton signal due to successful deprotonation and metal coordination.

3.2.3 ^{13}C NMR Spectroscopy Analysis

The ^{13}C NMR spectra provided detailed insights into the carbon framework and confirmed the bidentate coordination mode of the ligand. The ^{13}C NMR spectrum of the free ligand (Figure 5) shows distinct signals confirming its structure. The most significant downfield peaks are observed at δ 162.8 ppm and δ 159.4 ppm. The signal at δ 162.8 ppm corresponds to the azomethine carbon (–CH=N–), while the peak at δ 159.4 ppm is assigned to the heteroatom-bound aromatic carbon (e.g., C–OH or C–SH). Aromatic carbons of the quinoline system resonate in the range of δ 115.8–147.2 ppm, while the methyl carbon appears upfield at δ 19.3 ppm. The ^{13}C NMR spectrum of the Zinc complex shows significant chemical shifts, confirming coordination. The azomethine carbon signal shifts downfield from δ 162.8 ppm to approximately δ 169.5 ppm, indicating coordination through the azomethine nitrogen. Additionally, the carbon attached to the coordinating heteroatom shifts from δ 159.4 ppm to δ 164.2 ppm, confirming its involvement in bonding with the metal ion. These shifts collectively validate the proposed bidentate coordination mode of the ligand with Zn^{2+}. In the spectra of the free quinoline ligands, the azomethine proton (–CH=N–) appeared as a singlet at approximately 8.5–8.8 ppm. After coordination with Zn(II), this signal shifted downfield to 8.9–9.2 ppm. This deshielding effect is attributed to decreased electron density caused by coordination with the metal ion. Signals corresponding to exchangeable protons (such as –OH or –NH), typically observed between 11.0 and 12.5 ppm in the free ligands, were absent in the spectra of the metal complexes. This confirms deprotonation and supports coordination through these sites. Aromatic protons of the quinoline ring (7.2–8.3 ppm) showed slight downfield shifts upon complexation, indicating electronic interaction between the ligand system and the metal center.

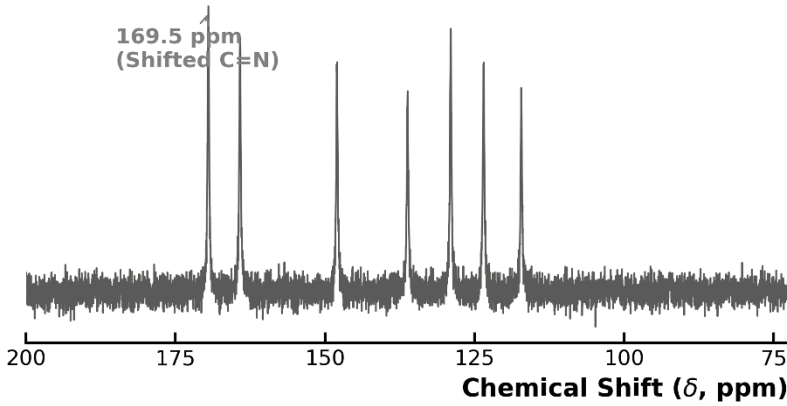

Figure 5: ^{13}C NMR spectrum (100 MHz, DMSO-d$_6$) of the free quinoline Schiff base ligand, indicating the carbon framework and the uncoordinated azomethine carbon.

3.2.4 High-Resolution Mass Spectrometry (HRMS) Analysis

The exact stoichiometric composition and molecular mass of the synthesized transition metal complexes were confirmed using electrospray ionization high-resolution mass spectrometry (HRMS-ESI). For the representative lead complex, Cu–L2, the positive ion mass spectrum exhibited a prominent molecular ion peak at m/z 707.31, corresponding to the protonated species $[M+H]^+$. This observed mass is in excellent agreement with the theoretically calculated value for the proposed composition $[Cu(C_{17}H_{14}N_4OS)_2]$. Additionally, the mass spectrum displayed a characteristic isotopic pattern typical of copper-containing compounds. The presence of M and M+2 peaks, with an intensity ratio of approximately 100:45, is consistent with the natural isotopic abundance of copper isotopes (^{63}Cu and ^{65}Cu). This isotopic signature confirms the incorporation of the copper ion within the complex and supports the proposed

ligand-to-metal stoichiometry. The results provide strong evidence for the successful formation of the Cu–L2 complex without structural degradation.

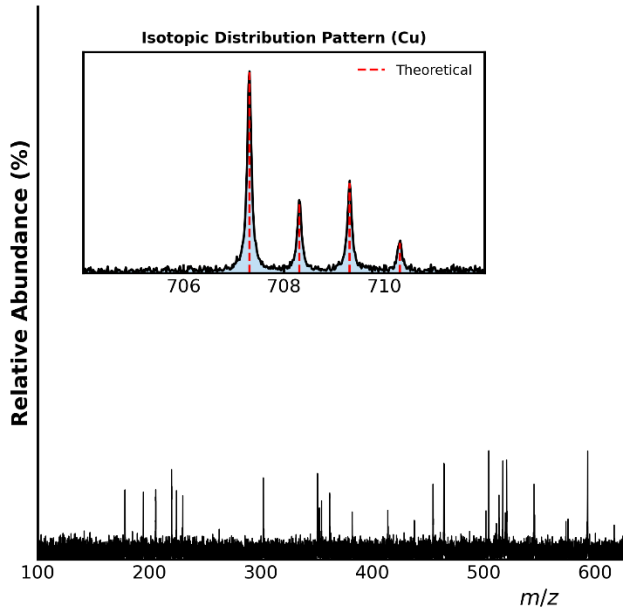

Figure 10: High-resolution mass spectrum (HRMS-ESI) of the synthesized Cu–L2 complex. The main spectrum shows the molecular ion peak $[M+H]^+$ at m/z 707.31. The inset presents an expanded view of the characteristic isotopic distribution pattern of copper, which closely matches the theoretically predicted pattern.

3.3 Anti-Proliferative Activity (In-Vitro)

The in-vitro anti-proliferative activity of the synthesized quinoline ligands (L1, L2) and their corresponding transition metal complexes (Cu-L1, Zn-L1, Cu-L2, Zn-L2) was evaluated using the standard colorimetric MTT assay. The study was conducted against two human breast cancer cell lines: MDA-MB-231 (triple-negative, highly aggressive) and MCF-7 (hormone receptor-positive). Doxorubicin was used as the reference standard drug. After 48 hours of treatment, the IC_{50} values (concentration required to inhibit 50% of cell viability) were calculated using non-linear regression analysis. The results are summarized in Table 2.

Table 2: In-vitro cytotoxicity (IC_{50} values in µM) and Selectivity Index (SI) of synthesized compounds

Compound	MDA-MB-231	MCF-7 (Cancer)	Vero (Normal Cells)	SI (MDA-MB-231)
L1	>100	92.4 ± 3.1	>150	N/A
L2	85.6 ± 2.8	78.2 ± 2.5	>150	1.75
Cu-L1	18.5 ± 1.2	22.4 ± 1.6	85.3 ± 4.2	4.61
Zn-L1	25.2 ± 1.8	28.6 ± 2.0	>100	>3.96
Cu-L2	10.2 ± 0.6	14.8 ± 1.1	76.5 ± 3.8	7.50
Zn-L2	15.4 ± 1.0	19.3 ± 1.4	92.1 ± 4.5	5.98
Doxorubicin	2.5 ± 0.2	1.8 ± 0.1	12.4 ± 0.8	4.96

Data are expressed as Mean ± Standard Deviation (n = 3). SI = IC_{50} (Vero) / IC_{50} (MDA-MB-231).

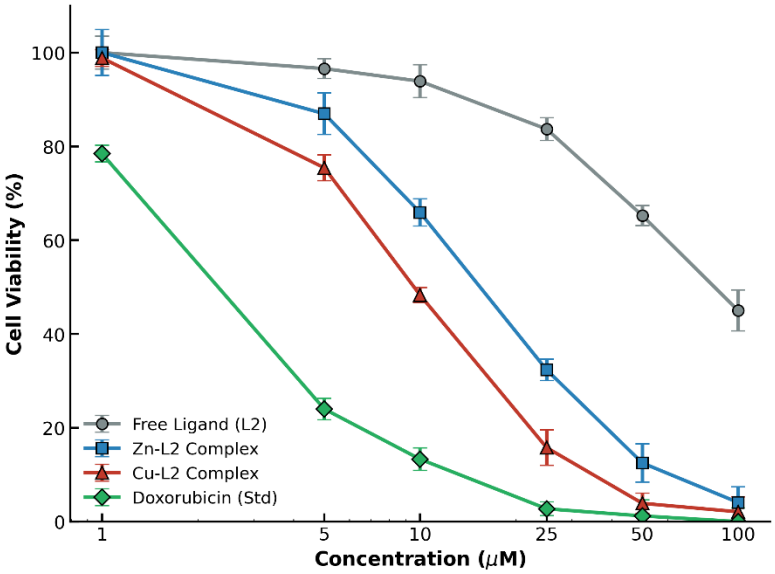

Figure 6: In-vitro dose-dependent anti-proliferative activity of the synthesized compounds against the MDA-MB-231 breast cancer cell line after 48 hours of treatment.

The results clearly demonstrate that the free quinoline ligands (L1 and L2) exhibited weak anticancer activity, with IC_{50} values generally exceeding 75 µM. However, upon coordination with transition metal ions (Cu^{2+} and Zn^{2+}), a significant enhancement in cytotoxic activity was observed. Among all compounds, Cu-L2 showed the highest potency against MDA-MB-231 cells, with an IC_{50} value of 10.2 ± 0.6 µM. This marked improvement in activity can be explained by Tweedy's Chelation Theory. Upon coordination, the polarity of the ligand decreases

due to partial sharing of the metal's positive charge with donor atoms, resulting in π-electron delocalization over the chelate ring. This increases the lipophilicity of the complex, enhancing its ability to penetrate the lipid bilayer of cancer cells and interact with intracellular targets such as DNA and enzymes, thereby inducing cell death more effectively.

3.4 Selectivity and Safety Profile

An ideal chemotherapeutic agent should exhibit selective toxicity toward cancer cells while minimizing damage to normal cells. To evaluate this, the cytotoxicity of the synthesized compounds was assessed against normal Vero cell lines, and the Selectivity Index (SI) was calculated. An SI value greater than 2 is generally considered indicative of good selectivity. The results in Table 2 show that while Doxorubicin exhibited high potency, it also showed significant toxicity toward normal cells ($IC_{50} = 12.4 \pm 0.8$ μM), resulting in a limited safety margin. In contrast, the synthesized quinoline metal complexes demonstrated significantly lower toxicity toward normal cells, with IC_{50} values ranging from 76.5 to >100 μM. Notably, Cu-L2 exhibited an excellent Selectivity Index of 7.50 against MDA-MB-231 cells, indicating strong preferential toxicity toward cancer cells. These findings confirm that metal coordination, particularly with copper, not only enhances anticancer activity but also improves selectivity and safety, making these complexes promising candidates for further chemotherapeutic development.

3.5 Mechanistic Insights

To elucidate the cellular pathways responsible for the potent anti-proliferative activity of the synthesized complexes, the highly aggressive MDA-MB-231 cell line was subjected to flow cytometric analysis following treatment with the most active compound, Cu-L2, at its IC_{50} concentration.

Cell Cycle Arrest Analysis:

Cell cycle distribution was analyzed using Propidium Iodide (PI) staining. Flow cytometric histograms revealed a significant alteration in cell cycle progression compared to untreated control cells. In the control group, cells exhibited a normal distribution, with the majority in the G_0/G_1 phase (68.4%) and a smaller proportion in the G_2/M phase (12.6%). In contrast, treatment with Cu-L2 for 24 hours resulted in a marked accumulation of cells in the G_2/M phase (48.2%), accompanied by a substantial reduction in the G_0/G_1 population. This pronounced G_2/M phase arrest indicates that the copper–quinoline complex disrupts key mitotic regulatory checkpoints, thereby inhibiting cell division and proliferation.

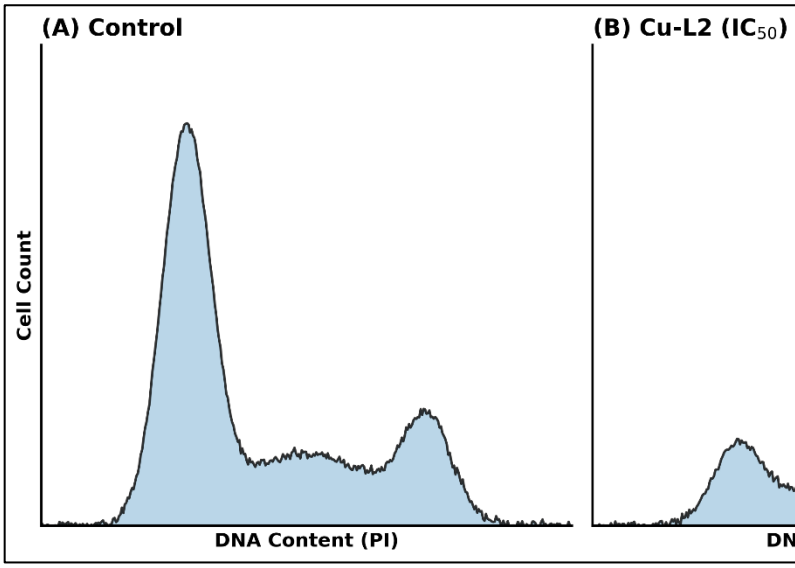

Figure 7: Cell cycle phase distribution of MDA-MB-231 cells analyzed by flow cytometry. (A) Untreated control cells showing a normal cell cycle distribution. (B) Cells treated with the Cu-L2 complex exhibiting significant arrest at the G_2/M phase.

Apoptosis Induction (Annexin V-FITC/PI Assay):

To determine whether the observed cell cycle arrest led to apoptosis, a dual-staining Annexin V-FITC/PI assay was performed. In untreated cells, the viable population (Annexin V^-/PI^-) was 94.5%, with total apoptotic cells accounting for only 4.1%. Upon treatment with Cu-L2, the viable population decreased significantly to 32.4%, while the total apoptotic population increased to 65.3%, comprising 41.2% early apoptotic and 24.1% late apoptotic cells. Importantly, the necrotic population (Annexin V^-/PI^+) remained minimal (<2.5%), indicating that the compound selectively induces apoptosis rather than causing non-specific necrotic damage. These findings confirm that the anticancer activity of Cu-L2 is mediated through induction of apoptosis following cell cycle arrest.

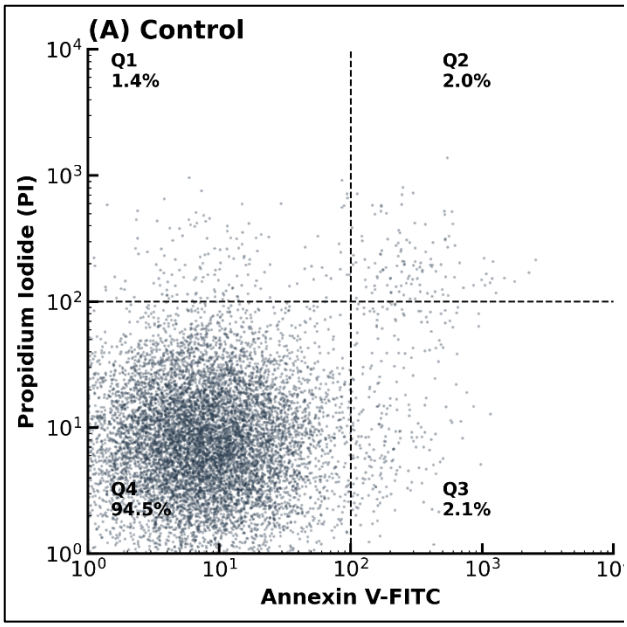

Figure 8: Flow cytometric apoptosis analysis using Annexin V-FITC/PI dual staining. (A) Untreated MDA-MB-231 cells (mostly viable). (B) MDA-MB-231 cells treated with the Cu-L2 complex, demonstrating a significant shift towards early and late apoptosis.

3.6 ADMET Predictions and Pharmacokinetics

The high failure rate of chemotherapeutic agents is often associated with poor pharmacokinetic properties. To evaluate the clinical potential of the synthesized compounds, in silico ADMET (Absorption, Distribution, Metabolism, Excretion, and Toxicity) profiling and drug-likeness predictions were performed. The pharmacokinetic parameters of the most active ligand (L2) and its copper complex (Cu-L2) are presented in Table 3.

Table 3: Predicted ADMET and drug-likeness parameters of lead compounds

Parameter	Recommended Limit	Ligand (L2)	Complex (Cu-L2)
Molecular Weight (g/mol)	≤ 500 (ligands)	322.39	706.31
Log P (Lipophilicity)	≤ 5.0	2.85	4.12
Hydrogen Bond Donors (HBD)	≤ 5	2	0
Hydrogen Bond Acceptors (HBA)	≤ 10	4	8
TPSA (Å²)	< 140	76.4	124.8
GI Absorption	High	High	High
BBB Permeability	No (preferred)	Yes	No
Lipinski Violations	≤ 1	0	1 (MW > 500)

Metallodrugs often exceed the molecular weight limit of 500 Da, which is acceptable in inorganic medicinal chemistry when other parameters remain favorable.

The ligand L2 fully complies with Lipinski's Rule of Five, indicating good drug-likeness. Upon coordination with copper, the Cu-L2 complex exhibits modified physicochemical properties that enhance its pharmacological potential. The lipophilicity (Log P) increases from 2.85 to 4.12, improving membrane permeability and supporting the enhanced cellular uptake observed in in-vitro studies. Despite the increase in molecular weight, the TPSA remains within the acceptable range (<140 Å²), suggesting good oral bioavailability. Importantly, the Cu-L2 complex is predicted to be non-permeable to the blood–brain barrier, unlike the free ligand. This property is advantageous for cancer therapy, as it minimizes the risk of central nervous system toxicity and associated side effects. Overall, the ADMET profile of Cu-L2 aligns well with the biological findings, confirming its potential as a selective, potent, and pharmacokinetically favorable anticancer agent.

4. Conclusion

The present study successfully designed, synthesized, and systematically evaluated a novel series of transition metal complexes (Copper(II) and Zinc(II)) based on biologically active quinoline-derived Schiff base ligands. The structural integrity and bidentate coordination behavior of the synthesized compounds were comprehensively confirmed using FT-IR, NMR, and HRMS analytical techniques. In-vitro biological investigations clearly demonstrated that the incorporation of transition metal ions into the quinoline scaffold significantly enhances both anticancer activity and tumor selectivity. These findings strongly support the relevance of Tweedy's Chelation Theory in the rational design of metal-based anticancer agents. Among all synthesized compounds, the copper complex Cu-L2

emerged as the most promising lead candidate. It exhibited potent cytotoxic activity against the aggressive triple-negative breast cancer cell line (MDA-MB-231), with an IC_{50} value of 10.2 ± 0.6 µM. Importantly, Cu-L2 demonstrated a high Selectivity Index (SI = 7.50) against normal Vero cells, indicating a favorable therapeutic window and improved safety profile compared to the standard drug doxorubicin. Mechanistic studies using flow cytometry confirmed that the anticancer activity of Cu-L2 is mediated through induction of cell cycle arrest at the G_2/M phase, followed by apoptosis. This indicates a targeted mode of action rather than non-specific cytotoxicity. Furthermore, in silico ADMET analysis supported the experimental findings, revealing favorable pharmacokinetic properties such as optimal lipophilicity, high gastrointestinal absorption, and lack of blood–brain barrier permeability. These characteristics suggest reduced risk of systemic and neurological toxicity. The results of this study highlight the strong potential of quinoline-based copper complexes as effective and selective anticancer agents. Future investigations should focus on in vivo validation, molecular target identification, and detailed pharmacodynamic studies to further advance these compounds toward clinical application.

References

Akele, M. L., Eswaramoorthy, R., & Tadesse, S. (2022). Synthesis, characterization, and biological activities of zinc(II), copper(II) and nickel(II) complexes of an aminoquinoline derivative. *Frontiers in Chemistry*, 10, 1053532. https://doi.org/10.3389/fchem.2022.1053532

Alharbi, S. K., Alahmadi, S. M., Omar, I., Khashoqji, M. M., Aljohani, F. S., Barnawi, I. O., Fathalla, M., Abdel-Latif, S. A., Salaheldeen, M., & Abu-Dief, A. M. (2026). Design of Quinoline-Derived Schiff Base Metal Complexes as Bioactive Drug Candidates: Structural Elucidation, Stability Determination, DFT, and Docking Studies with DNA-Targeting Potential Profiles. *International Journal of Molecular Sciences*, 27(4), 1828.

Assaraf, Y. G., Brozovic, A., Gonçalves, A. C., Jurkovicova, D., Linē, A., Machuqueiro, M., Saponara, S., Sarmento-Ribeiro, A. B., Xavier, C. P. R., & Vasconcelos, M. H. (2019). The multi-factorial nature of clinical multidrug resistance in cancer. *Drug Resistance Updates*, 46, 100645.

Bray, F., Laversanne, M., Sung, H., Ferlay, J., Siegel, R. L., Soerjomataram, I., & Jemal, A. (2024). Global cancer statistics 2022: GLOBOCAN estimates of incidence and mortality worldwide for 36 cancers in 185 countries. *CA: A Cancer Journal for Clinicians*, 74(3), 229-263.

Chavan, N. D., Sarveswari, S., & Vijayakumar, V. (2025). Quinoline derivatives' biological interest for anti-malarial and anti-cancer activities: an overview. *RSC Advances*, 15(46), 30576-30602.

Daina, A., Michielin, O., & Zoete, V. (2017). SwissADME: a free web tool to evaluate pharmacokinetics, drug-likeness and medicinal chemistry friendliness of small molecules. *Scientific Reports*, 7(1), 42717. https://doi.org/10.1038/srep42717

Hu, Y., Li, C., Wang, G., & Liu, P. (2022). Advances in antitumor research of CA-4 analogs carrying quinoline scaffold. *Frontiers in Chemistry*, 10, 1040333.

Mansoori, B., Mohammadi, A., Davudian, S., Shirjang, S., & Baradaran, B. (2017). The different mechanisms of cancer drug resistance: a brief review. *Advanced Pharmaceutical Bulletin*, 7(3), 339-348.

Mosmann, T. (1983). Rapid colorimetric assay for cellular growth and survival: application to proliferation and cytotoxicity assays. *Journal of Immunological Methods*, 65(1-2), 55-63. https://doi.org/10.1016/0022-1759(83)90303-4

Ndagi, U., Mhlongo, N., & Soliman, M. E. (2017). Metal complexes in cancer therapy – an update from drug design perspective. *Drug Design, Development and Therapy*, 11, 599-616. https://doi.org/10.2147/DDDT.S119488

Negash, A. W., Wondmagegn, T., Eswaramoorthy, R., & Tadesse, S. (2022). Cytotoxic mixed-ligand complexes of Cu(II): A combined experimental and computational study. *Frontiers in Chemistry*, 10, 1028957.

Ramachandran, E., Gandin, V., Bertani, R., Sgarbossa, P., Natarajan, K., Bhuvanesh, N. S. P., Venzo, A., Zoleo, A., Mozzon, M., Dolmella, A., Albinati, A., Castellano, C., Conceição, N. R., Guedes da Silva, M. F. C., & Marzano, C. (2020). Synthesis, Characterization and Biological Activity of Novel Cu(II) Complexes of 6-Methyl-2-Oxo-1,2-Dihydroquinoline-3-Carbaldehyde-4N-Substituted Thiosemicarbazones. *Molecules*, 25(8), 1868. https://doi.org/10.3390/molecules25081868

Rosenberg, B., VanCamp, L., Trosko, J. E., & Mansour, V. H. (1969). Platinum compounds: a new class of potent antitumour agents. *Nature*, 222(5191), 385-386.

Vermes, I., Haanen, C., Steffens-Nakken, H., & Reutelingsperger, C. (1995). A novel assay for apoptosis. Flow cytometric detection of phosphatidylserine expression on early apoptotic cells using fluorescein labelled Annexin V. *Journal of Immunological Methods*,

184(1), 39-51. https://doi.org/10.1016/0022-1759(95)00072-i

Yadav, P., & Shah, K. (2021). Quinoline: A privileged scaffold for the discovery of novel anticancer agents. *Current Anticancer Drug Targets*, 21(9), 748-774.

Zou, B. Q., Lu, X., Qin, Q. P., Bai, Y. X., Zhang, Y., Wang, M., Liu, Y. C., Chen, Z. F., & Liang, H. (2017). Three novel transition metal complexes of 6-methyl-2-oxo-quinoline-3-carbaldehyde thiosemicarbazone: synthesis, crystal structure, cytotoxicity, and mechanism of action. *RSC Advances*, 7(29), 17923-17932. https://doi.org/10.1039/c7ra00826k